Supporting Information

$BiVO_4$ quantum dots decorated $BiPO_4$ nanorods 0 D/1 D heterojunction for enhanced Visible-Light-Driven photocatalysis

Boyuan Li[a†], Zhenhua Cao[b†], Shixuan Wang[a], Qiang Wei[a], Zhurui Shen*[a]*

Corresponding author: *Zhurui Shen*; Adress: Key Laboratory of Advanced Ceramic and Machining Technology, Department of Materials Science and Engineering, Tianjin University, Yaguan Road 135, Jinnan District, Tianjin 300350, P. R. China; Tel: 0086-13702014847; Email: shenzhurui@tju.edu.cn.

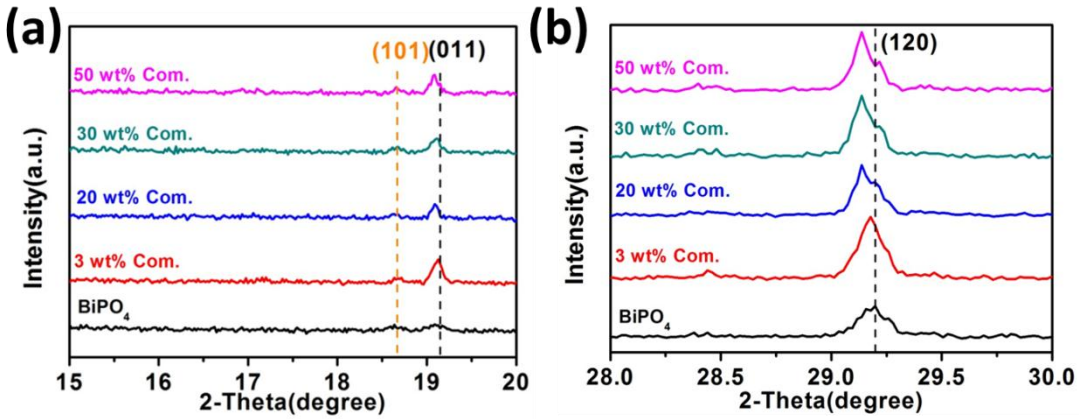

Fig. S1 (a) peak positions of the (101) (011) plane in the range of θ =15.0–20.0 °. (b) peak positions of the (120) plane in the range of θ =28.0–30.0 °.

With the increase of $BiVO_4$, it reached the most preferential crystallorgraphic orientation along the (101) direction. This was probably caused by the selective adsorption of Bi^{3+} on certain facet of $BiPO_4$. In addition to the preferential crystallographic orientation, a careful comparison of the (011) and (120) showed that the peak position of $BiPO_4$ with different $BiVO_4$ contents shifted slightly toward a lower 2-Theta (degree) value. According to Bragg' s Law: $n\lambda=2d\sin\theta$, where d is the distance between crystal planes of (h k l), λ is the X-ray wavelength, and θ is the diffraction angle of the crystal plane (h k l). The decrease of 2θ in $BiPO_4$ should result from the increase in lattice parameters (d (011) and (120) value), verifying that $BiVO_4$

has been successfully embedded into $BiPO_4$ and bonded with $BiPO_4$. The result could also be confirmed by FT-IR, XPS and TEM.

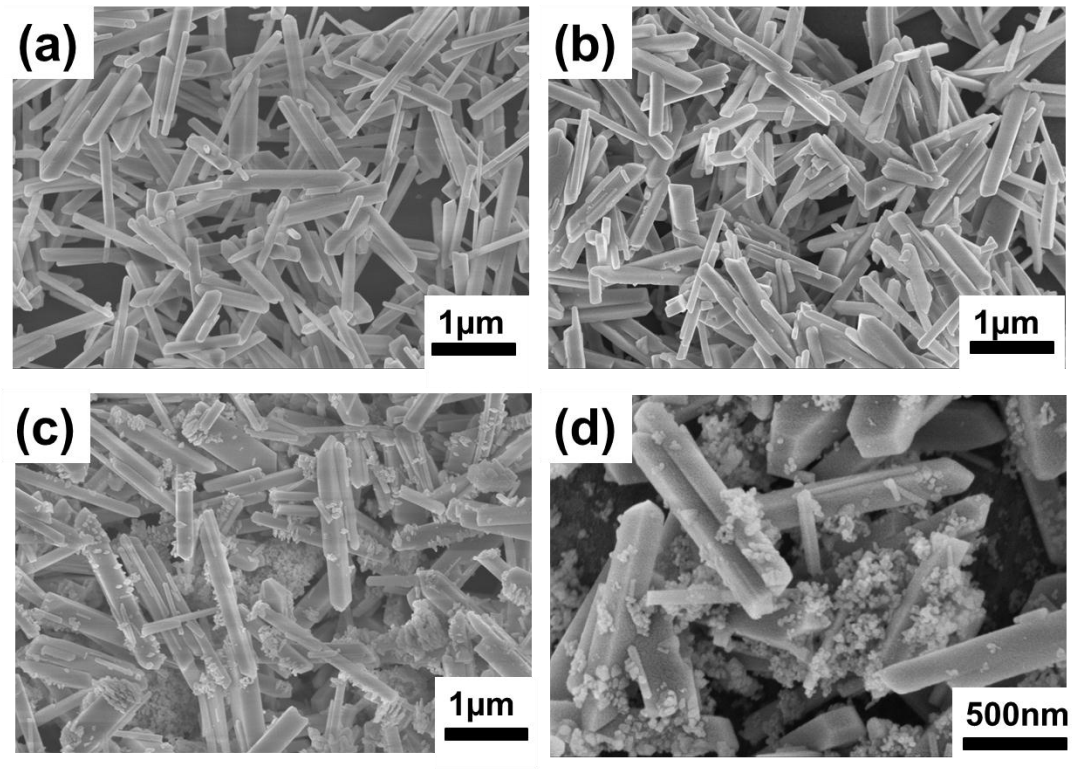

Fig. S2. SEM images of samples. (a) $BiPO_4$; (b) 3 wt% $BiVO_4/BiPO_4$; (c) 20 wt% $BiVO_4/BiPO_4$; (d) 30 wt% $BiVO_4/BiPO_4$.

The 3 wt% $BiVO_4/BiPO_4$ has almost no particles because the mass ratio of $BiVO_4$ is too low to find (Fig. S2 (b)). The amount of particles is apparently increased with $BiVO_4$ added.

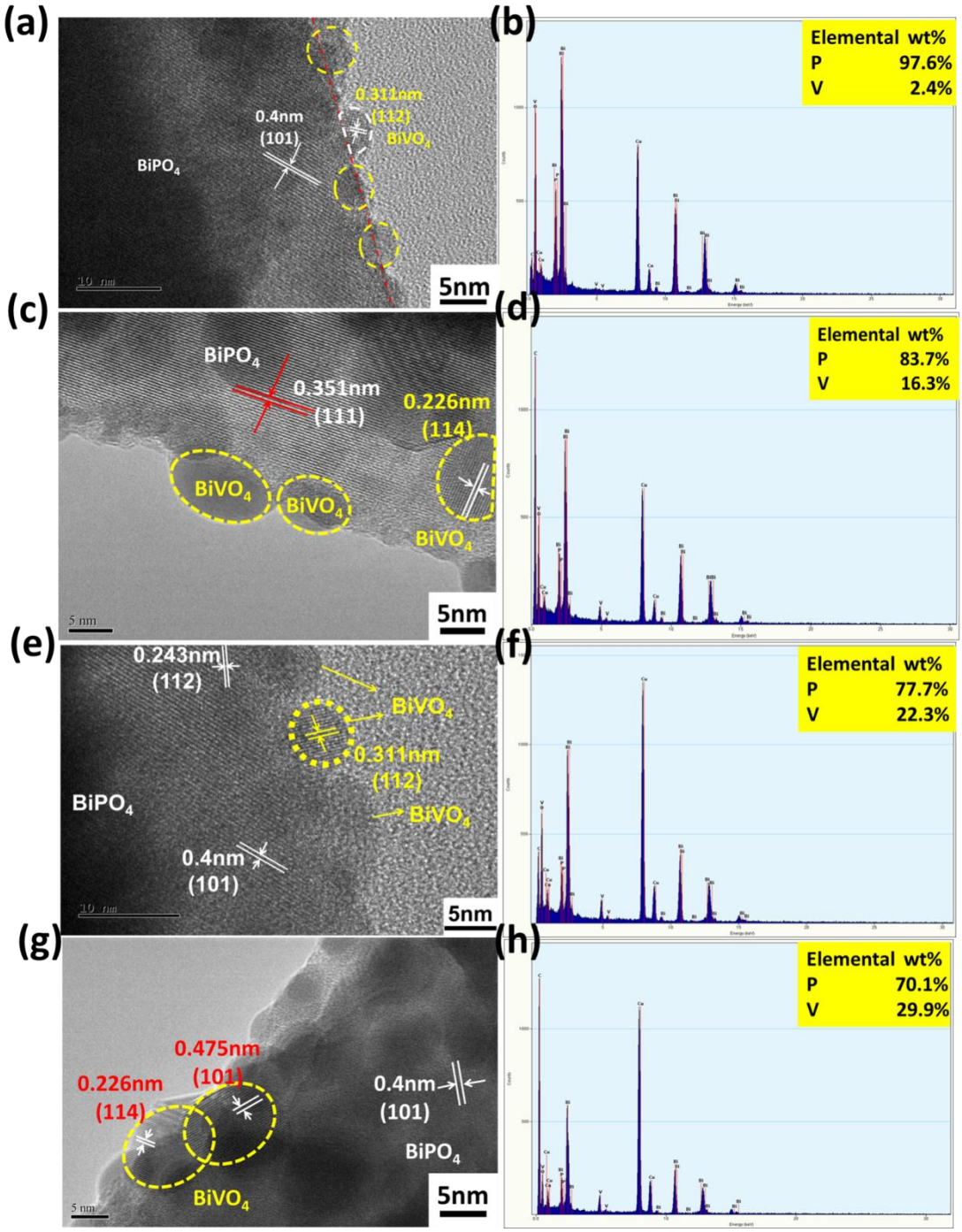

Fig. S3 HRTEM images of (a) 3 wt% $BiVO_4/BiPO_4$, (c) 20 wt% $BiVO_4/BiPO_4$, (e) 30 wt% $BiVO_4/BiPO_4$ and (g) 50 wt% $BiVO_4/BiPO_4$. EDAX spectrum of (b) 3 wt% $BiVO_4/BiPO_4$, (d) 20 wt% $BiVO_4/BiPO_4$, (f) 30 wt% $BiVO_4/BiPO_4$ and (h) 50 wt% $BiVO_4/BiPO_4$.

In terms of $BiVO_4$ combined with $BiPO_4$ to form nanocomposite, the HRTEM and EDAX of 3 wt% $BiVO_4/BiPO_4$, 20 wt% $BiVO_4/BiPO_4$, 30 wt% $BiVO_4/BiPO_4$ and 50 wt% $BiVO_4/BiPO_4$ have been shown in Fig. S3. $BiVO_4$ formed quantum dots, dispersed on the surface of $BiPO_4$. From the Fig. S3a, c, e, g, it can be seen that a well interfacial contact between $BiVO_4$ and $BiPO_4$. The lattice fringes of the marked

particles can be assigned to the (112) (Fig. S1a), (114) (Fig. S1c), (112) (Fig. S1e) and (114) (101) (Fig. S1g) facets of $BiVO_4$. The heterojunction has well formed between $BiVO_4$ and $BiPO_4$. With the mass ratio of $BiVO_4$ increasing, the QDs on the surface of $BiPO_4$ have also been added. The EDAX shows the elements of Bi, P, V, O, indicating that the composite consisted of $BiPO_4$ and $BiVO_4$. From EDAX analysis, the mass ratio of V/P was approximately in correspondence with 3 wt%, 20wt% 30 wt% and 50 wt% (Fig. S3b, d, f, h). The results above proved that $BiVO_4$ formed a kind of nanocomposite with $BiPO_4$ rather than being present as a separate.

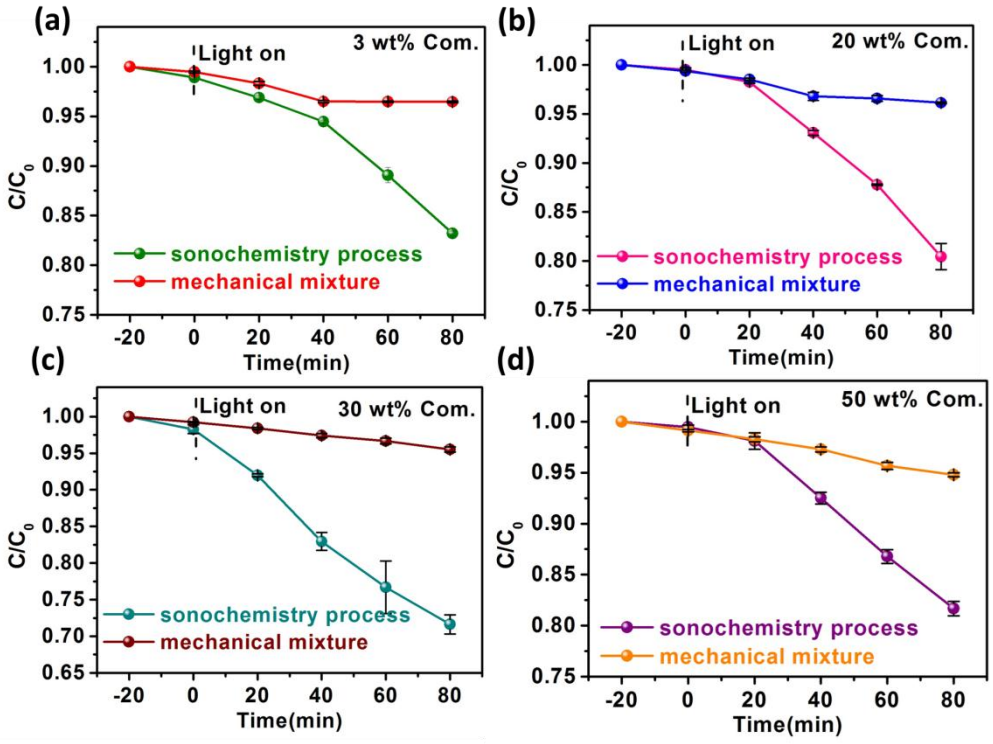

Fig. S4 Photo-degradation of Rh B of (a) 3 wt% $BiVO_4/BiPO_4$ by sonochemistry process and by mechanical mixture; (b) 20 wt% $BiVO_4/BiPO_4$ by sonochemistry process and by mechanical mixture; (c) 30 wt% $BiVO_4/BiPO_4$ by sonochemistry process and by mechanical mixture; (d) 50 wt% $BiVO_4/BiPO_4$ by sonochemistry process and by mechanical mixture.

In the meantime, the performance of four composites prepared by sonochemistry process was compared with those by mechanical mixture (Fig. S4). We tested the photocatalytic activity of 3 wt% $BiVO_4/BiPO_4$ prepared by sonochemistry process and mechanical mixture, showing 17 % and 3.6 % degradation, respectively. The degradation of 20 wt% $BiVO_4/BiPO_4$, 30 wt% $BiVO_4/BiPO_4$ and 50 wt% $BiVO_4/BiPO_4$ was 3.8 %, 4.2 % and 5.3 %, respectively. The composites prepared by mechanical mixture almost showed the same degradation efficiency with pristine $BiVO_4$ (6 %). With $BiVO_4$ added, the degradation efficiency increased slightly from 3.6 % to 5. 3%， because $BiPO_4$ couldn't be excited under visible light. Therefore, $BiVO_4$ is present in the nanocomposite.

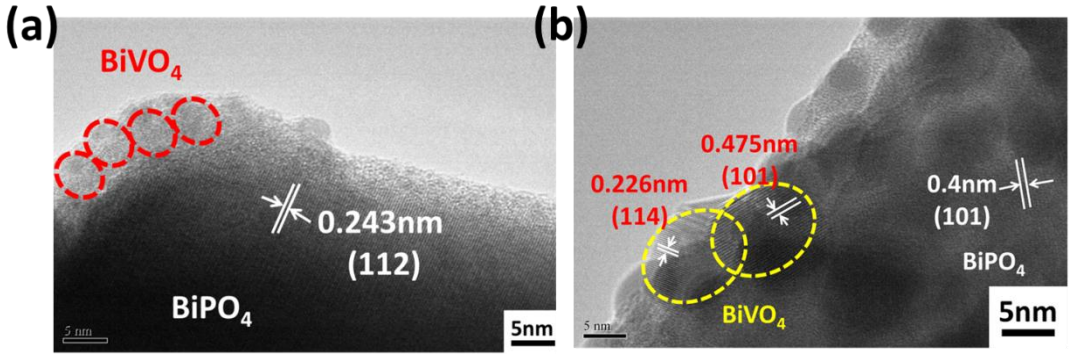

Fig. S5 HRTEM images of 50 wt% $BiVO_4/BiPO_4$ (a) before and (b) after sonochemical process.

As shown in Fig. S5, the heterojunction of $BiVO_4$ QDs/$BiPO_4$ nanorods before and after sonochemical process have similar morphology at low magnification. However, the HRTEM images show that the $BiVO_4$ QDs before sonication are amorphous, while the ones after sonication are crystalline. This result indicates that the sonochemical process promotes the crystallization of $BiVO_4$ QDs.

Table S1 k=-ln(C/C$_0$) of photocatalyst

Samples	k(min^{-1})
$BiVO_4$	0.000555
$BiPO_4$	0.000417
3 wt% Com.	0.00181
20 wt% Com.	0.00217
30 wt% Com.	0.00346
50 wt% Com.	0.00217
Dark Control	0.0000927
Light Control	0.0000972

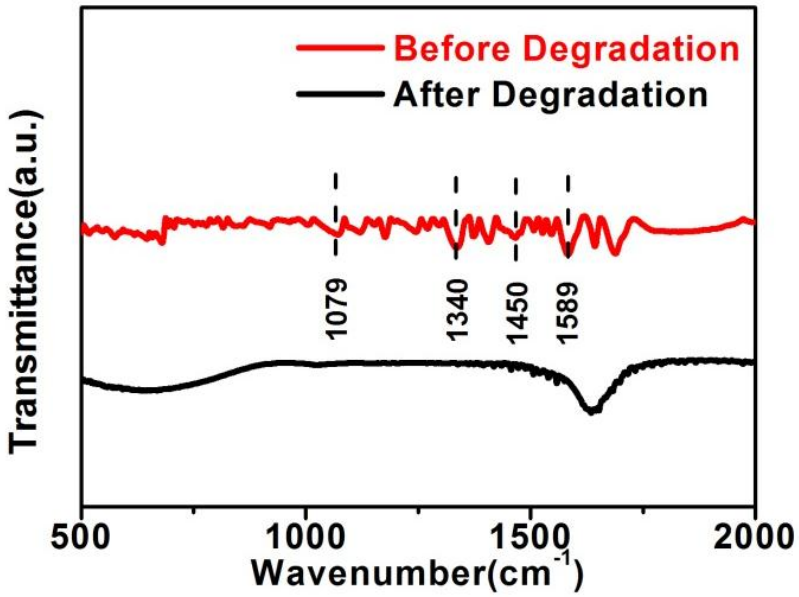

Fig. S6 FT-IR spectra of 30 wt% $BiVO_4$/$BiPO_4$ photocatalyst before and after the photodegradation test.

In the Fig. S6, 1589 cm^{-1}, 1340 cm^{-1}, 1180 cm^{-1} and 1079 cm^{-1} represent the stretching vibrational peaks of the benzene ring molecular framework in Rh B molecules, which are the C-CH_3 symmetry bending vibration peak and the stretching vibration of the ether linkage bond C-O-C before degrading Rh B. It is clearly seen that there is only the stretching vibrational peak of 1630 cm^{-1}, indicating –OH is left in the solution which means there is no organic substance after degradation. The result of FT-IR consistent with TOC verifies again that 30 wt% $BiVO_4$/$BiPO_4$ has a wonderful mineralization process during the photodegradation.

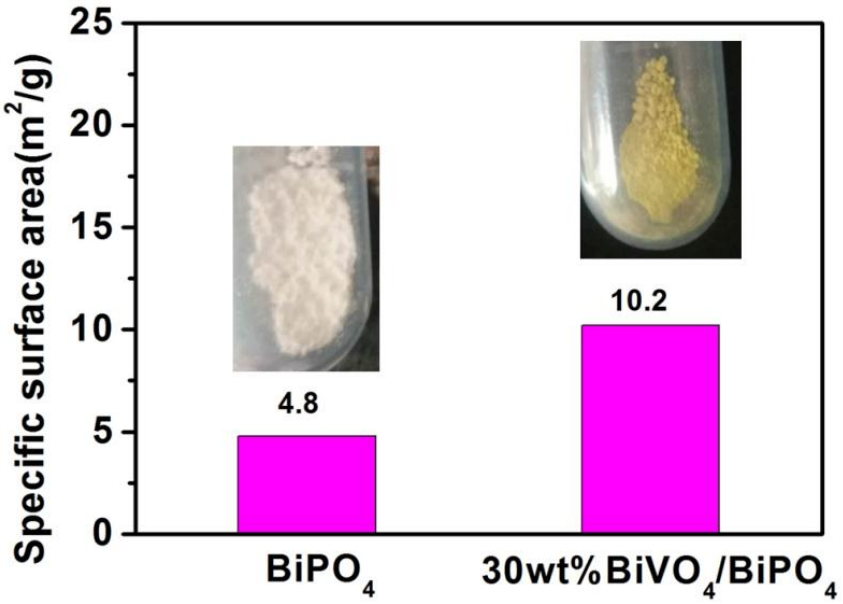

Fig. S7 Specific surface area of $BiPO_4$ and 30 wt% $BiVO_4/BiPO_4$.

The specific surface area of 30 wt% $BiVO_4/BiPO_4$ is virtually almost the same as that of pure $BiPO_4$ (4.8 m^2 g^{-1} for pure $BiPO_4$ and 10.2 m^2 g^{-1} for 30 wt% $BiVO_4/BiPO_4$, Fig. S7). The inner left side of the Figure S3 is the pure $BiPO_4$ powder and the right one is the 30 wt% $BiVO_4/BiPO_4$.

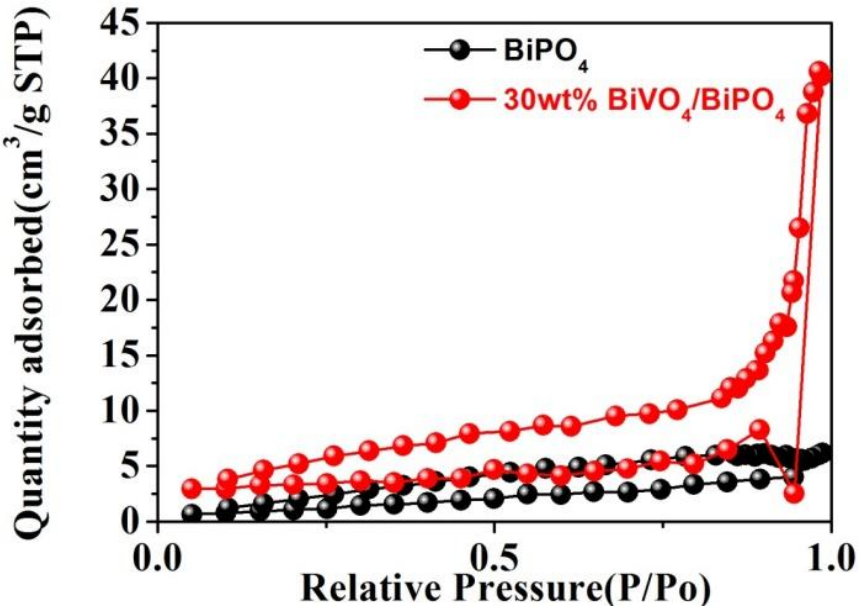

Fig. S8 N_2 adsorption-desorption isotherms of $BiPO_4$ and 30 wt% $BiVO_4/BiPO_4$.

The N_2 adsorption-desorption isotherms of 30 wt% $BiVO_4/BiPO_4$ shows definitely higher quantity adsorb than pure $BiPO_4$ does, which means mesoporous increase after adding $BiVO_4$. However, none of the two curves are closed so that the composites are not composed of mesoporous at all.

Table S2 The fitting parameters of the Randles equivalent circuit

Samples	R_s(ohm)	R_{ct}(ohm)	$C_{ct}(10^{-4})$
$BiPO_4$	10.480	2713	1.433
$BiVO_4$	9.335	2202	1.384
$BiVO_4/BiPO_4$	10.150	1339	1.918

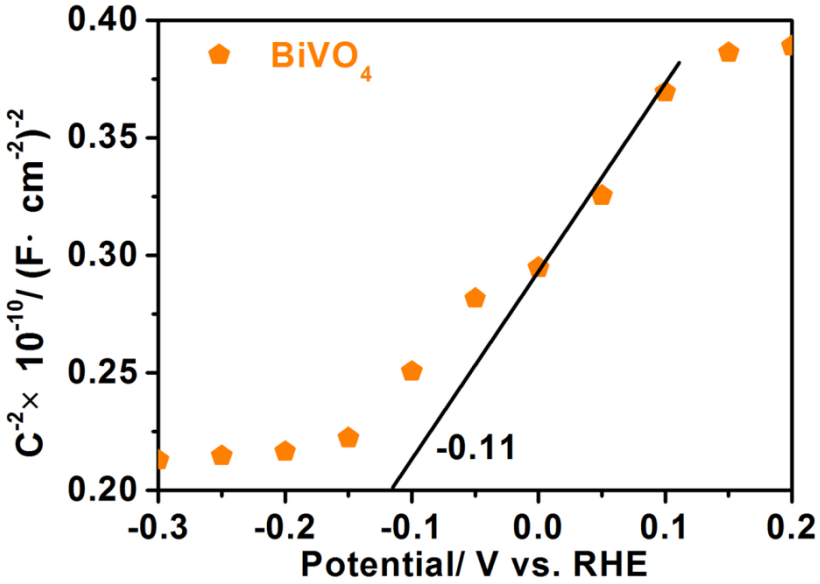

Fig. S9 Mott-Schottky plot of $BiVO_4$.